Nonlinear electrical transport through artificial grain-boundary junctions in $La_{0.7}Ca_{0.3}MnO_3$ epitaxial thin films

Mandar Paranjape,* J. Mitra, and A. K. Raychaudhuri†
Department of Physics, Indian Institute of Science, Bangalore 560 012, India

N. K. Todd, N. D. Mathur, and M. G. Blamire
Department of Materials Science and Metallurgy, Cambridge University, Cambridge CB2 3QZ, United Kingdom

We report investigation of non-linear electronic transport through artificial grain-boundary junctions made on epitaxial films of $La_{0.7}Ca_{0.3}MnO_3$ on bicrystal $SrTiO_3$ substrates. The experiments carried out over the temperature range 4.2 K–300 K in magnetic field up to 3 T allow us to identify some of the conduction mechanisms that may give rise to nonlinear transport in these grain boundary junctions. The nonlinear transport is associated with multistep inelastic processes in the grain-boundary region, which is moderately affected by the applied magnetic field. However the primary effect of the magnetic field is to enhance the zero-bias conductance $[G_0=(dI/dV)_{V=0}]$. The dominant voltage dependent contribution to the dynamic conductance $(G=dI/dV)$ comes from a term of the type $V^{4/3}$ at lower temperatures. Other voltage dependent contributions to G, which are of higher order in V, appear only for $T\geqslant 75$ K. In addition we found a contribution to G arising from a $V^{0.5}$ term, which is likely to arise from the disordered region around the grain boundary (GB). The magnetoresistance in the GB depends on the bias used and it decreases at higher bias. The bias dependence is found to be reduced as temperature is increased. We discuss the physical origins of the various contributions to the nonlinear conduction.

I. INTRODUCTION

Electrical transport in rare-earth manganites showing colossal magnetoresistance (CMR) has been a topic of intense research in the last decade. In these materials the transport through the grain boundary (GB) is different from that in the bulk.[1–3] The two most prominent features in the GB transport are as follows: (a) The magnetoresistance (MR) in the GB was found to be more at $T\ll T_C$ (T_C is the ferromagnetic transition temperature and the GB-MR decreases as $T\rightarrow T_C$ from below) and (b) the low-field magnetoresistance response (LFMR) is much pronounced in the GBs compared to that in the bulk of the crystallite. These two behaviors are in sharp contrast to those observed in the bulk, where the (high-field) MR peaks near the ferromagnetic transition temperature T_C. Also the MR in the bulk is much less at low field. The LFMR in GB has been investigated extensively due to their potential technological applications following the first GB device reported on $La_{1-x}Ca_xMnO_3, x\approx 0.3$ (LCMO) films on $SrTiO_3$ (STO) substrates with bicrystal junction.[4] The GB transport in CMR materials is generally probed through two types of experiments. The first method is to study transport in polycrystalline materials with monodispersed grains and well formed grain boundaries.[1,2,5,6,7] This method, however, needs a model to separate out the contribution of the GB and the bulk. The second method is to study the transport in artificial GB created in an epitaxial film of the CMR oxide.[4,8–13] This method gives more definitive results because the transport in the GB and that in the bulk of the film can be effectively separated. To probe the nature of the transport through GB's in CMR oxides, many research groups have carried out investigations on various systems such as tunnel junctions,[3] step edge junctions,[9] artificial grain boundaries on epitaxial thin film using bicrystal substrate,[4,8,11–14] mechanically induced grain boundaries,[9,10] and spin-flip junction devices.[15] We will call such a device containing an artificial grain boundary a grain boundary junction (GBJ). The transport through the GBJ is generally modeled as a junction where the GB is the barrier and the bulk of the film adjoining the GB are the two electrodes. The two electrodes are spin-polarized metals ($T<T_c$). The nature of the transport is thus mainly dominated by the physical nature of the barrier region, its width, and the junction that the barrier forms with the spin-polarized electrodes. A number of mechanisms (strictly speaking scenarios) have been proposed to explain the LFMR in the GB and its temperature dependence. Most of the proposed mechanisms are based on tunneling through the GB. Briefly, the mechanisms proposed are the spin-polarized tunneling via nonmagnetic impurity,[1,4–6] tunneling via magnetic impurity,[16] spin-polarized inelastic tunneling through a spin-glass-like layer,[10] and magnetic polarization of the GB region.[17] Recent experiments proposed multistep impurity mediated transport through the GB.[11,12] While most of the experiments on GBJ investigated LFMR, the temperature dependence of LFMR, and hysteresis behavior, there are recent investigations that have measured the nonlinear transport through the GBJ (nonlinear I-V).[12,13,18]

In this investigation we address the question of nonlinear transport through such junctions and the effects of temperature and magnetic field on them. We find the nonlinear junction conductance through the GB, which arises from various inelastic as well as elastic processes and dominates the transport at finite bias. These are moderately affected by the applied magnetic field, whereas the zero-bias conductance is enhanced by a large amount in a magnetic field.

II. EXPERIMENT

In this paper we report measurements done on GBJ's formed by artificial grain boundary in the epitaxial LCMO thin films grown on symmetrical bicrystal STO substrates. GBJ devices were made from patterned thin films of LCMO grown by pulsed laser deposition on STO bicrystal substrates (45° misorientation). The details of the growth of the thin films on the bicrystal substrates, their patterning to form devices and measurement of their resistance have been described previously.[4,13] We have studied two types of devices. The first device is made from a 200-nm-thick film which is strain relaxed (GBJ200) and the second device is made from a 40-nm film (GBJ40) which is essentially strained due to substrate. Details about their microstructure as well as their LFMR response have been published previously.[13] These devices show large MR ($\approx$50%) in a field as small as 20 mT. In this study we have used a large Wheatstone bridge geometry with 19 meanders crossing the grain boundary. The current path is inclined at an angle of 12° with the grain boundary. The symmetry of the bridge structure ensures that all resistance contributions balance to zero except those arising from the GB. However, deviation from perfect balance of the arms of the Wheatstone bridge can lead to contribution from bulk of the film close to T_P, where resistivity ρ_{bulk} reaches a peak. The I-V measurements were carried out by passing direct current through current leads $I+$ and $I-$ and measuring voltage drop across voltage leads $V+$ and $V-$ as a function of temperature and applied magnetic field. The output resistance in this configuration is $R_{GB}/2$ if the arms of the bridge are properly balanced. An off-balance contribution (R_{off}), which contains contribution from the bulk of the film, shows up closer to T_C, as will be shown later. Total R_{GB} contains contribution from the 19 meanders of the bridge arm. The voltage drop across the arm is $V \approx 19V_{meander}$, where $V_{meander}$ is the drop across each crossing. The maximum power dissipated was less than 1 mW at the highest applied bias. The applied magnetic field was parallel to the GB if not otherwise stated. The resistance R, MR, I-V, and dynamic conductance [$G(=dI/dV)$ vs V] measurements were done in a liquid-helium cryostat with a superconducting magnet in zero field and in $H=3$ T as a function of temperature ranging from 4.2 K to 300 K. The magnet was warmed up to room temperature prior to each run.

III. RESULTS

Figures 1(a) and 2(a) show resistance vs temperature for the two GBJ's. In Fig. 1(a) we show resistance of GBJ200, which has a value of nearly 18 kΩ and it peaks at 273 K (defined as T_P). T_P is similar to that of the 200-nm pristine film grown on the same substrate. The resistivity of the pristine film is shown in the same graph. In Fig. 2(a) we show R vs T for GBJ40. This device is made from a thinner film, which is essentially strained due to substrate. GBJ40 shows resistance, at T_P, two orders higher than that of GBJ200. The resistance peaks around 198 K which is very close to T_P of the bare film, also shown in Fig. 2(a). The ratio of resistance at T_P to the resistance at 4.2 K ($R_{PEAK}/R_{4.2\,\mathrm{K}}$) is $\approx$8 for GBJ200 and $\approx$3.5 for GBJ40. The corresponding values for the pristine epitaxial films are much larger. This clearly brings out the role of GB in increasing resistance at lower

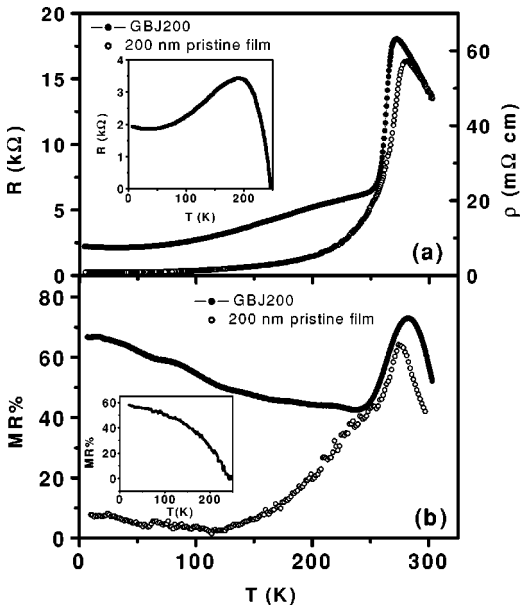

FIG. 1. (a) Grain-boundary resistance as a function of temperature for a 200-nm device (open circles) along with resistivity of pristine film (open squares). Inset shows corrected resistance of the device (see text). (b) MR at 5 T as a function of temperature for a 200-nm device (open circles) as well as that of pristine film. Inset shows corrected MR of the device (see text).

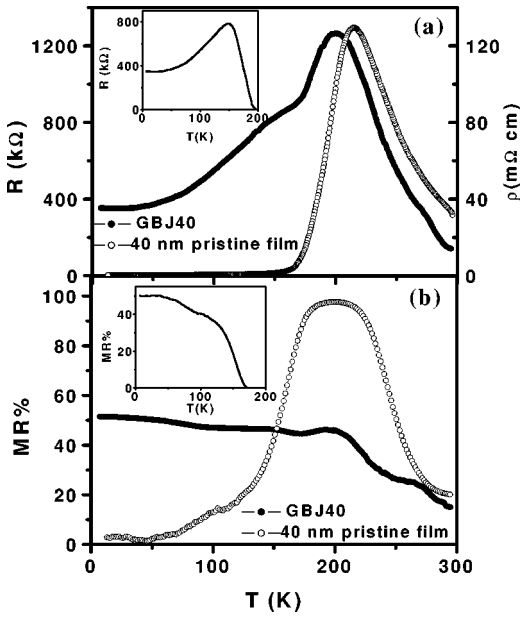

FIG. 2. (a) Grain-boundary resistance as a function of temperature for a 40-nm device (open circles) along with resistivity of pristine film (open squares). Inset shows corrected resistance of the device (see text). (b) MR at 5 T as a function of temperature for a 40-nm device (open circles) as well as that of pristine film. Inset shows corrected MR of the device (see text).

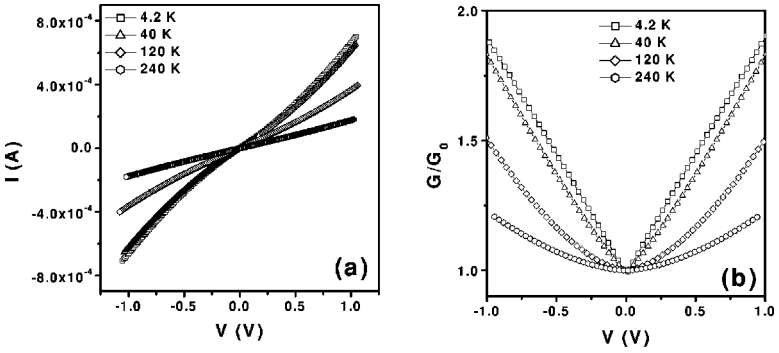

FIG. 3. (a) I-V curves of a 200-nm device taken at various temperatures in a zero magnetic field. (b) The normalized dynamic conductance G/G_0 vs V curves obtained from the curves shown in (a).

temperatures ($T \ll T_P$). The resistance values of the GBJ's show peak near T_P of the pristine films. As stated earlier this is due to off-balance of the bridge. To approximately account for this we follow the following procedure. We write $R \approx R_{GB} + R_{eff}$, where $R_{eff} = \xi R_{bulk}$, R_{bulk} is the resistivity of the pristine film and ξ is the scale factor which accounts for the meanders off-balance. We then adjust ξ in a such a way that the observed value of R is reproduced in the transition region using values of the resistivities of the pristine films. Similar procedure is followed for the MR. The corrected resistances of the GBJ's arising from the GB only are shown in the insets of Figs. 1(a) and 2(a). The resistance of the GB is very similar to what is seen in polycrystalline pellets.

In Figs. 1(b) and 2(b) we also show the MR as a function of temperature T in a field of 5 T. The MR for the GBJ200 at 5 T is $\approx 60\%$ as $T \to 0$ and it decreases as T increases up to 220 K, eventually peaking at T_P showing MR value of 71%. In the same graph we show the MR of the pristine film (200 nm) grown under the same condition. The MR in the film peaks near T_P but is negligible below 150 K. GBJ40 shows MR at 4.2 K of about 36% and remains more or less flat up to 140 K. MR shows a shallow peak around T_P (38%) and decreases on further increase in temperature. The MR of a pristine film is shown for comparison. It has broad peak near T_P but it is also negligible below 150 K. In insets of Figs. 1(b) and 2(b) we show the MR of the GBJ's after correcting the off-balance signal. One can see that the GB MR is maximum at the lowest temperature and decreases as temperature is increased.

Figure 3(a) shows I-V curves of GBJ200 in zero field at some representative temperatures. We show data in a temperature range $T < T_P$. Above T_P, I-V curves become linear. It is evident from the figure that the current-voltage characteristics are nonlinear in nature and the nonlinearity decreases as the temperature is increased. The corresponding normalized dynamic conductance data (G/G_0, where $G = dI/dV$) obtained by numerical differentiation of the I-V curves are shown in Fig. 3(b). The G/G_0-V curves are symmetric. The zero bias conductance G_0 [$= G(V=0)$] decreases as a function of temperature as T increases. Figures 4(a) and 4(b) show the corresponding data at $H = 3$ T. The applied magnetic field enhances the zero-bias conductance since the GB has a negative MR. The bias dependent part of the conductivity [$\Delta G(V) = G_V - G_0$] does not change substantially in 3 T applied magnetic field at lower temperatures ($T < 100$ K). At higher temperatures there is a noticeable reduction of $\Delta G(V)$. We quantify these in subsequent parts. The I-V and dynamic conductance curves, both in zero field and in 3 T magnetic field for the sample GBJ40, are qualitatively similar to that of GBJ200, although they differ in quantitative details. However, to avoid duplicity we do not show the data for the sample GBJ40.

The GB-MR has an interesting bias dependence. To show this we plot in Fig. 5, the conductance ratio $\xi_V \equiv G_V(3\text{ T})/G_V(0\text{ T})$ as a function of temperature for four values of the bias voltage $V \approx 0$, 0.2, 0.5, and 0.7 V for GBJ200. $\xi_V > 1$ would imply negative MR. The field of 3 T is much higher than the field of any hysteretic and anisotropic regime which in these devices is below 200 mT. It can be seen that as the bias is increased, ξ_V at a given temperature decreases significantly at low temperatures. At 4.2 K, ξ_V decreases as much as 25% at a bias value of 0.7 V compared to that of the zero bias. However, the bias dependence decreases as the temperature increases. The bias dependence decreases substantially in the region $T \approx 75$ K–100 K and for $T > 150$ K the bias dependence of ξ_V is negligible. This observation brings out the fact that contribution of nonlinear

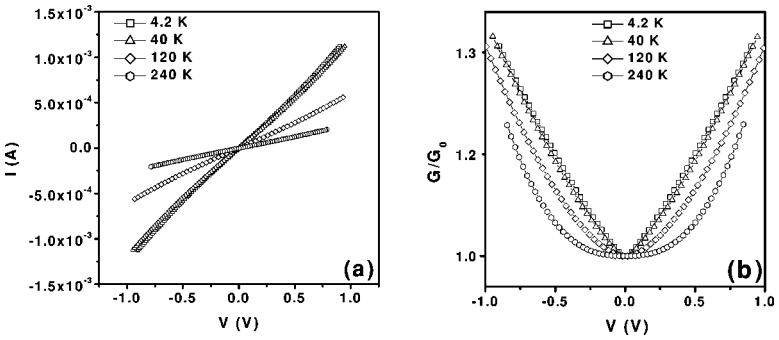

FIG. 4. (a) I-V curves of a 200-nm device at various temperatures in 3 T magnetic field applied parallel to the grain boundary. (b) The normalized dynamic conductance G/G_0 vs V curves obtained from the curves shown in (a).

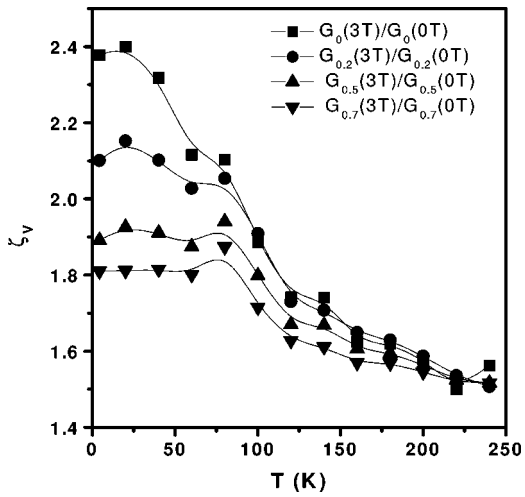

FIG. 5. The conductance ratio $\xi_V = G_V(3\text{ T})/G_V(0\text{ T})$ of a 200-nm device as a function of T for three values of the bias voltage $V \approx 0$, 0.2, 0.5, and 0.7 V.

conduction decreases as the temperature is increased. We also note that the temperature dependence of ξ_V [MR $=(\xi_V - 1)/\xi_V$] is substantial for $V=0$ for $T<100$ K. In contrast, ξ_V for finite V has rather small temperature dependence for $T<75$ K. For $T>100$ K for all bias values, ξ_V has nearly the same temperature dependence. This we feel is an important observation from the view point of device application. It is seen that in the temperature range 75 K–100 K there is a distinct change in the transport mechanism through the device. We see below that this is linked to a changeover of conduction mechanism through the GB at $T \approx 75$ K as an additional channel for inelastic transport through the GB opens up. Similar decrease in GB-MR with increasing bias has also been seen before.[12,19] A GB device has to be operated at a finite bias and a higher bias is desirable because this will reduce the noise in the device. However, a higher bias will reduce the MR. Thus an optimal choice of the bias is needed.

IV. DISCUSSION

a. The nature of nonlinearity—An empirical approach. The bias dependence of the dynamic conductance (G vs V) taken at different T and H are fitted to the empirical expression

$$G(V,T) = G_0(T) + \Delta G(V,T) = G_0(T) + G_\alpha(T)|V|^\alpha. \quad (1)$$

Equation (1) is a two-parameter relation that quantifies the nonlinearity through the exponent α and G_α, which is a measure of the weight of the nonlinear transport. G_α, α, and G_0 are all functions of T and H. In Fig. 6 we show the temperature dependence of the three parameters as a function of T for $H=0$ T and $H=3$ T for GBJ200. G_0 and G_α decrease and α increases monotonically with increasing T in zero field. The temperature dependence of α in $H=0$ T has a number of distinct features. $\alpha<1$ at the lowest T and increases steadily as T increases, reaching the value of ≈ 1.8 at around 100 K. It saturates to ≈ 1.8–1.9 above 100 K.

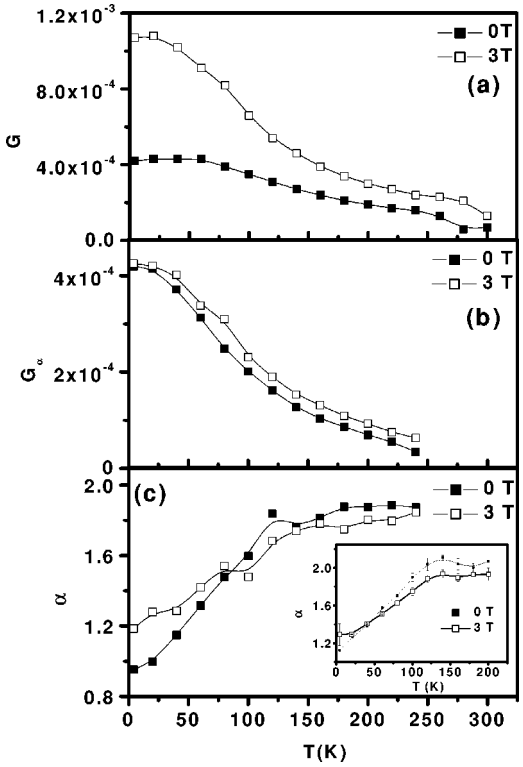

FIG. 6. The temperature dependence of the three parameters G_0, α, and G_α in zero field and $H=3$ T for a 200-nm device. The inset shows the temperature dependence of the parameter α in zero field and $H=3$ T for a 40-nm device.

In Fig. 6 we also show the temperature dependence of G_0, G_α, and α in a magnetic field of 3 T. As expected G_0 is enhanced in the magnetic field and this is the negative MR shown by the junction close to zero bias. However, there are interesting changes in α and G_α. For $T<75$ K, $\alpha(3\text{ T})$ is enhanced and it is significant at lower temperatures. It is larger than $\alpha(0\text{ T})$ in this temperature range. At ≈ 75 K there is a crossover and $\alpha(3\text{ T})$ is slightly lower than $\alpha(0\text{ T})$. $\alpha(3$ T) also reaches a steady value of ≈ 1.7–1.8 at around 120 K.

The temperature and magnetic-field dependences of G_0, G_α, and α seen in GBJ40 are similar to those of GBJ200 and are not plotted. Particularly the values of α in zero field as well as in 3 T are similar for both devices. This is shown in the inset of Fig. 6. In GBJ40, α is somewhat larger than that in GBJ200 and the field dependence is less pronounced. As in GBJ200, $\alpha(3\text{ T})$ is larger than $\alpha(0\text{ T})$ at lower T and after a crossover at ≈ 50 K stays lower than $\alpha(0$ T). At higher temperature ($T>125$ K) both α values reach a constant value close to 2.

In Fig. 7, $\alpha(0\text{ T})$ obtained in two other investigations[10,18] are plotted with that obtained in this investigation. (So far we have not come across any published reports where α and G_α have been obtained in a magnetic field.) The investigation in Ref. 9 was done on $La_{0.7}Ca_{0.3}MnO_3/LaAlO_3$ devices but the GBJ was a step array junction in contrast to the bicrystal junctions used in our investigation. The investigation in Ref. 18 was done on $La_{0.67}Ba_{0.33}MnO_3/SrTiO_3$, with GBJ made on bicrystal substrate. Though the three GBJ's are different,

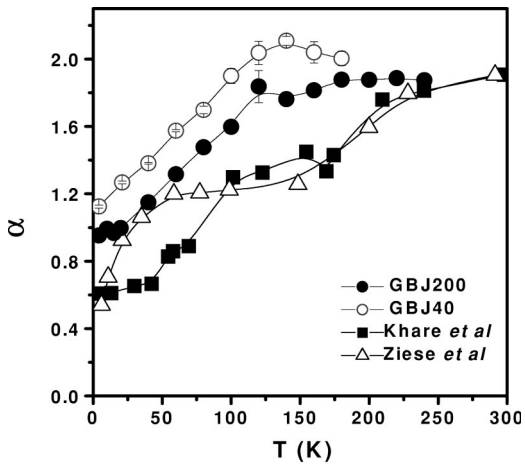

FIG. 7. A comparison of the temperature dependence of the parameter α in zero field for both devices along with Ziese *et al.* (Ref. 9) and Khare *et al.* (Ref. 18).

one can see certain common trends in all of them. $\alpha(0\ \mathrm{T})$ seen in all the three investigations show two distinct regimes. At lower temperatures ($T<100$ K) $\alpha(0\ \mathrm{T})$ starts increasing steadily with temperature. At higher temperatures in our junction, α reaches a steady value close to 1.8–2 at $T>125$–150 K. In the junctions of Refs. 9 and 18 there is an additional plateau at $\alpha\approx 1.2$–$1.3(50\ \mathrm{K}<T<200\ \mathrm{K})$ before it reaches the limiting slope of nearly 2 at higher temperatures $T>200$ K. We interpret this behavior as due to distinct transport mechanisms that operate in the GBJ. We discuss these mechanisms in the following section. It is likely that all the mechanisms occur simultaneously although one of them wins over the others in a given temperature range. However, the relative weight of the different mechanisms, the exact values of $\alpha(0\ \mathrm{T})$, and the exact temperature ranges where the crossovers occur will depend on the details of the physical nature of the junctions as well as on the materials which have been used to make the junction.

b. Models of GB transport. In this section we briefly highlight the salient features of the transport mechanisms that could explain the nonlinear *I-V* curves seen in the GBJ. The models have been developed in the context of transport through tunnel junctions or junctions comprising two metallic electrodes with a barrier separating them. The applicability of these theories is based on the basic assumption that the GBJ can be thought of as junction with metallic electrodes with a barrier separating them. The expected behavior will depend on the physical nature of the electrodes, the barrier, and the presence or absence of scattering in the barrier regions. In general, the tunneling through a junction with rectangular energy barrier gives rise to a parabolic dependence of G on V at low voltages such that[19,20]

$$G(V)=G_0+G_2|V|^2. \tag{2}$$

In this equation the transport is an elastic process and the voltage dependence arises from the voltage dependence of the tunneling barrier transmission probability. The coefficient G_2 depends on parameters related to the energy barrier. Usually the contribution of the voltage dependent term is much weaker than the zero-bias conductance G_0. It is a zero-temperature theory and does not include any aspect of spin-polarized transport. This effect is not affected by magnetic field unless the barrier is significantly modified by the field.

In case the electrodes of a tunneling junction are disordered the conductance gets a characteristic dependence on voltage given as[21,22]

$$G(V,T)=G_0(T)+G_{0.5}(T)|V|^{0.5}. \tag{3}$$

The characteristic dependence is a manifestation of electron-electron interaction in weakly localized disordered solids.[21] This coefficient $G_{0.5}$ is a strong function of temperature T and it decreases rapidly as T is increased. This has been experimentally seen in disordered metallic alloys as well as in disordered metallic oxides[22] at low temperatures ($T<10$ K). In this case the junction transport has weak dependence on the magnetic field to the extent that the quantum corrections are suppressed by the magnetic field. Presence of this term would mean that the region around the junction is disordered and it is different from the bulk of the film. We discuss this later.

A model by Jullière[23] is widely used in the context of spin-polarized transport through magnetic tunnel junction. However, this model does not include contributions from inelastic tunneling. In this model the tunneling resistance between two ferromagnetic metal layers separated by a thin insulating barrier depends on the relative orientation of the magnetization and the electron-spin polarization in each layer. The model is essentially a two-current model, one for each spin direction. The two-current model assumes that the two spin species of electrons tunnel elastically. This model gives us a way to calculate the relative current in the spin channels and thus obtain an estimation of the degree of spin polarization. The model has been extended to include inelastic contribution to explain the reduction of the GB-MR at higher bias.[12]

Glazman and Matveev[24] (GM) proposed a theory for multistep tunneling for conduction in disordered solid. This theory has been developed for inelastic tunneling across amorphous films and not for junctions with a barrier in the conventional sense. However, given the fact that the GB is a junction whose ''barrier'' thickness d (typically $\geqslant$ few nanometers or more) is much wider than that in conventional tunnel junctions ($d\approx 1-10$ nm), the applicability of the GM model may be justified. This particular issue will be discussed later on. The GM model has given a generalized expression for voltage dependent dynamic conductance. In our experiments $\mathrm{eV}\gg k_BT$ is satisfied for most parts of the *I-V* curves, except the range very close to the zero-bias region. In such a case the model gives a voltage dependent conductance which one can write as[24]

$$G(V)=G_0+G_{4/3}|V|^{4/3}+G_{5/2}|V|^{5/2}+\cdots, \tag{4}$$

where the first term G_0 includes the elastic tunneling and tunneling via single-impurity step. $G_{4/3}$ is the contribution by tunneling via two impurity states. The tunneling involving more impurity sites will have higher-order terms. The coef-

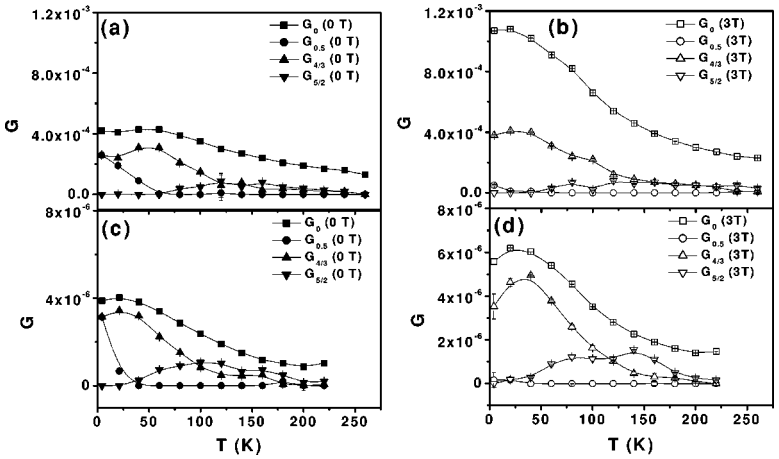

FIG. 8. (a) The temperature dependence of the coefficients (G's) in zero field and (b) $H=3$ T for a 200-nm device, (c) the temperature dependence of the coefficients (G's) in zero field, and (d) $H=3$ T for a 40-nm device [see text and Eq. (7)].

ficients depend on the radius of the localized states, their density, and the barrier thickness d.

A recent theory[16] specifically addresses the question of inelastic spin-flip scattering in magnetic junctions. It calculates the contribution of bulk magnons as well as antiferromagnetic surface magnons at the junction regions between two dissimilar magnetic materials. The contribution due to the bulk magnons gives rise to a nonlinear dynamic conductance in the low-bias region,

$$G(V)=G_0+G_{3/2}|V|^{3/2}, \tag{5}$$

with the temperature dependence of the MR which decreases as T increases at low temperatures. The contribution due to surface magnons gives rise to a bias dependent conductivity

$$G(V)=G_0+G_2|V|^2. \tag{6}$$

In this case the nonlinearity of the transport arises from the spin-flip process. As a result, application of magnetic field which suppresses the spin-flip scattering will significantly suppress the nonlinear transport. In this section we briefly summarized the models available to understand the nature of nonlinear transport in GBJ. In the following section we use these models to analyze the measurements done on the GBJs. The change of the nonlinear terms of the junction transport in a magnetic field can be used as a tool to check the presence of spin-dependent processes in these junctions that cause the nonlinear transport.

c. Analysis of GB transport data application of the models. Most of the investigations on GBJ address the issue of LFMR and its dependence on temperature. However, some of the past investigations looked into the particular issue of nonlinear transport. The investigations by Zeise *et al.*[9,10] and Khare *et al.*[18], as stated earlier, analyzed the data using the empirical relation given in Eq. (1). The effect of applied magnetic field was not investigated. Similar GBJ samples have been investigated by Klein *et al.*[11] and Höfener *et al.*[12] who explained their data using the GM theory. From the empirical analysis done in Sec. IV a and Fig. 6, one can note the following.

(1) The nonlinear term $\Delta G(V)$ arises due to contributions from a number of processes.

(2) Predominant exponent for the nonlinear term is close to 1.7–1.9 over most of the temperature range for $T>125$ K. We will see below that this arises because of a contribution from a term with higher power (V^n, $n>2$). This term makes substantial contribution for $T\geqslant 75$ K and the relative contribution from this term increases as T is increased. However, at low temperatures ($T<50$ K) there are contributions from other process with voltage dependence V^m with $m<1$. These contributions decrease as T is increased.

(3) The effect of magnetic field is to enhance the zero-bias term G_0 predominantly. Also, the other terms that give rise to nonlinear transport are affected by the magnetic field though weakly.

In view of the discussions in the preceding section we propose that the nonlinear contribution $\Delta G(V,T,H)$ consists of contributions from three processes, all of which occur in parallel and we write this as

$$G(V,H,T)=G_0+G_{0.5}|V|^{0.5}+G_{4/3}|V|^{4/3}+G_{5/2}|V|^{5/2}, \tag{7}$$

where the zero-bias conductance G_0 consists of two parts. One part is the elastic tunneling giving rise to the GB-MR and another part is the contribution of the tunneling through a single impurity site as envisaged in the GM model. The $G_{0.5}$ term is due to the disorder effect as expressed in Eq. (3). $G_{4/3}$ and $G_{5/2}$ are the contributions from two- and three-step tunneling, respectively, of the GM model [see Eq. (4)]. The higher-order terms are neglected due to increasingly smaller contribution. The predominant dependence of the field is from the G_0 term. In view of the absence of large dependence of the voltage dependent part on the magnetic field we did not include any spin-dependent contributions as envisaged in Eqs. (5) and (6).

We fit the observed G-V data (both for $H=0$ and 3 T) to Eq. (7) over the whole voltage range and at all temperatures (4.2 K to T_P). One can obtain excellent fit with fit error $<\pm 0.5\%$. The fit parameters, namely, the term G_0 and the coefficients $G_{0.5}$, $G_{4/3}$, and $G_{5/2}$ are shown in Fig. 8 for both GBJ's in $H=0$ and $H=3$ T. The dominant term in this region is evidently G_0, which contains the elastic term as well the single step tunneling. The contribution of the $V^{0.5}$ term in Eq. (7), although very small compared to the G_0 and $G_{4/3}$

terms, is needed to improve the quality of the fit close to the zero bias region particularly at low temperatures. This term is also needed to explain the appearance of $\alpha<1$ at low temperatures as shown in Fig. 6. However, it decreases very rapidly as T increases and becomes negligible for $T>40$ K. Interestingly this term is suppressed by the magnetic field and is absent for $H=3$ T data for both samples. This explains the enhancement of the observed α at low temperatures in a magnetic field (see Fig. 6).

The main nonlinear contribution at low temperatures comes from the $V^{4/3}$ term, which arises from the multistep tunneling. This term is significant at lower temperatures ($T<50$ K). It decreases rapidly above 75 K. It shows broad peak around $T\approx 25$ K for both GBJ200 and GBJ40. The coefficient $G_{4/3}$ is enhanced moderately in the magnetic field at low temperatures, implying that the impurities involved in the multiple-step tunneling can be magnetic. The coefficient $G_{5/2}$ is almost negligible for $T<75$ K but assumes a finite value beyond that and dominates at higher T. The $|V|^{5/2}$ term comes from a process involving three steps. This being a higher-order process will involve higher-energy process which we believe is operative when the temperature is increased. The change in the nonlinear transport seen in the temperature range around $T\approx 50$ K–75 K is due to crossover of the relative contributions of these two terms. The contribution of this term makes $\alpha\rightarrow 2$ at $T>125$ K. We conclude that in this device spin-dependent processes do contribute to the nonlinear conduction through the GB but the substantial effect of the magnetic field is due to the zero-bias term. The nonlinear transport (which has a much weaker magnetic-field dependence) arises from a multistep process as envisaged in the GM theory with a contribution arising from the disordered region around the GB. We are in general agreement with the observations and conclusions of Höfener *et al.*[12] for the data taken at $H=0$ T. The applicability of the GM model and contribution of the $V^{0.5}$ term in the $G(V)$ data point to certain characteristics of the GB. It is not a sharp tunnel junction, as in most artificially fabricated magnetic tunnel junctions (MTJ's). One would expect no or much weaker inelastic scattering in a sharp junction. This will make the GM model inapplicable. Thus the applicability of the GM model would clearly signify that the GB junction is very different from the MTJ. Here the junction has a width $\gg$ mean free path of electron. In this context we refer to Soh *et al.*[25] Using micro-x-ray probe they showed that the region around the GB has a different lattice constant from the bulk of the film, and this change occurs in the scale of a micrometer. One would therefore argue that the electronic transport through the GB will be affected by this layer significantly. This modified region around the GB is likely to have significant disorder which contributes to the $V^{0.5}$ term in the tunneling process at low temperatures. We also note that the inelastic process coming from multistep tunneling, giving rise to the nonlinear transport, has much suppressed the dependence on magnetic field compared to G_0. The field dependence is expected to come from the spin-induced alignment/polarization of these impurity/scattering centers that give rise to a multistep process. Absence of a strong-field dependence will imply that either most of these steps are nonmagnetic or they have random spin orientation locked in space by local anisotropy.

A comparison between the GBJ's made on the two films shows that though they show qualitatively similar behavior there are significant quantitative differences. The relative contribution of the nonlinear terms is definitely much larger for GBJ40 compared to that of GBJ200. The magnetic field also has a relatively stronger dependence on GBJ40. The difference in the two devices is mainly to the extent of intrinsic strain in them.[26] GBJ40 is made from the uniformly strained film, whereas GBJ200 is made from strain relaxed film. We would expect that as a result of the strain in the film of GBJ40, the region around the GB is more affected by the strain and provides more sites for multiple-step tunneling in comparison to the same region in GBJ200.

V. CONCLUSION

To summarize our findings, we have studied nonlinear electrical transport through artificial grain-boundary devices made of $La_{0.7}Ca_{0.3}MnO_3$ grown on bicrystal $SrTiO_3$ substrate by pulsed laser ablation. We specifically investigated the dynamic conductance vs applied bias over the temperature range 4.2 K–300 K and in a magnetic field up to 3 T. The primary magnetic-field dependence is on the zero-bias conductance, which is strongly enhanced by the magnetic field. We find that the nonlinear transport is dominated mainly by two processes. The processes are moderately affected by the magnetic field. From the analysis of the nonlinear transport we suggest that the transport through the GB is not only affected by the physical junction but also by a finite length of the film around the GB that has different properties from the bulk.

ACKNOWLEDGMENTS

A.K.R. wants to acknowledge DST for a sponsored project. M.P. and J.M. want to acknowledge CSIR for financial support. The work was carried out under UK-India Joint Science and Technology Program. Part of this work was funded by the EPSRC of the UK and the Royal Society.

*Email address: mandar@physics.iisc.ernet.in

†Email address: arup@physics.iisc.ernet.in

[1] R. Mahesh, R. Mahendiran, A.K. Raychaudhuri, and C.N.R. Rao, Appl. Phys. Lett. **68**, 2291 (1996).

[2] H.Y. Hwang, S.W. Cheong, N.P. Ong, and B. Batlogg, Phys. Rev. Lett. **77**, 2041 (1996).

[3] X.W. Li, Yu Lu, G.Q. Gong, G. Xiao, A. Gupta, P. Lecocur, J.Z. Sun, Y.Y. Wang, and V.P. Dravid, J. Appl. Phys. **81**, 5509 (1997).

[4] N.D. Mathur, G. Burnell, S.P. Isaac, T.J. Jackson, B.-S. Teo, J.L. MacManus-Driscoll, L.F. Cohen, J.E. Evetts, and M.G. Blamire, Nature (London) **387**, 266 (1997).

[5] A. Gupta, G.Q. Gong, G. Xiao, P.R. Duncombe, P. Lecoeur, P. Trouilloud, Y.Y. Wang, V.P. Dravid, and J.Z. Sun, Phys. Rev. B **54**, R15 629 (1996).

[6] L. Balcells, J. Fontcuberta, B. Martinez, and X. Obradors, Phys. Rev. B **58**, R14 697 (1998).
[7] X. Liu, Z. Jiao, K. Nakamura, T. Hatano, and Y. Zeng, J. Appl. Phys. **87**, 2431 (2000).
[8] K. Steenbeck, T. Eick, K. Kirsch, H.G. Schmidt, and E. Steinbeib, Appl. Phys. Lett. **73**, 2506 (1998).
[9] M. Ziese, G. Heydon, R. Hohne, P. Esquinazi, and J. Dienelt, Appl. Phys. Lett. **74**, 1481 (1999).
[10] M. Ziese, Phys. Rev. B **60**, R738 (1999).
[11] J. Klein, C. Hofener, S. Uhlenbruck, L. Alff, B. Buchner, and R. Gross, Europhys. Lett. **47**, 371 (1999).
[12] C. Höfener, J.B. Philipp, J. Klein, L. Alff, A. Marx, B. Buchner, and R. Gross, Europhys. Lett. **50**, 681 (2000).
[13] N.K. Todd, N.D. Mathur, S.P. Issac, J.E. Evetts, and M.G. Blamire, J. Appl. Phys. **85**, 7263 (1999).
[14] D.J. Miller, Y.K. Lin, V. Vlasko-Vlasov, and U. Welp, J. Appl. Phys. **87**, 6758 (2000).
[15] C. Srinitiwarawong and M. Ziese, Appl. Phys. Lett. **73**, 1140 (1998).
[16] F. Guinea, Phys. Rev. B **58**, 9212 (1998).
[17] J.E. Evetts, M.G. Blamire, N.D. Mathur, S.P. Isaac, B.-S. Teo, L.F. Cohen, and J.L. MacManus-Drisscoll, Philos. Trans. R. Soc. London, Ser. A **356**, 1593 (1998).
[18] N. Khare, U.P. Moharil, A.K. Gupta, A.K. Raychaudhuri, S.P. Pai, and R. Pinto, Appl. Phys. Lett. **81**, 325 (2002).
[19] W. Westerburg, F. Martin, S. Freiedrich, M. Maier, and G. Jakob, J. Appl. Phys. **86**, 2173 (1999).
[20] J.G. Simmons, J. Appl. Phys. **34**, 1793 (1963).
[21] P.A. Lee and T.V. Ramakrishnan, Rev. Mod. Phys. **57**, 287 (1985).
[22] A.K. Raychaudhuri, K.P. Rajeev, H. Srikanth, and N. Gayathri, Phys. Rev. B **51**, 7421 (1995).
[23] M. Julliere, Phys. Lett. A **54**, 225 (1975).
[24] L.I. Glazman and K.A. Matveev, Sov. Phys. JETP **67**, 1276 (1988).
[25] Y. Soh, P.G. Evans, Z. Cai, B. Lai, C.-Y. Kim, G. Aeppli, N.D. Mathur, M.G. Blamire, and E.D. Isaacs, J. Appl. Phys. **91**, 7742 (2002).
[26] Mandar Paranjape, A.K. Raychaudhuri, N.D. Mathur, and M.G. Blamire, Phys. Rev. B **67**, 214415 (2003).